Journal of Materials Chemistry A

PAPER

View Article Online
View Journal | View Issue

Cite this: J. Mater. Chem. A, 2019, 7, 26586

Supported palladium membrane reactor architecture for electrocatalytic hydrogenation†

Roxanna S. Delima, [ab] Rebecca S. Sherbo, [c] David J. Dvorak, [b] Aiko Kurimoto [c] and Curtis P. Berlinguette *[abcd]

Received 22nd July 2019
Accepted 29th October 2019

DOI: 10.1039/c9ta07957b

rsc.li/materials-a

Electrolytic palladium membrane reactors offer a means to perform hydrogenation chemistry utilizing electrolytically produced hydrogen derived from water instead of hydrogen gas. While previous embodiments of these reactors employed thick (≥25 μm) palladium foil membranes, we report here that the amount of palladium can be reduced by depositing a thin (1–2 μm) layer of palladium onto a porous polytetrafluoroethylene (PTFE) support. The supported palladium membrane can be designed to ensure the fast diffusion of reagent and hydrogen to the palladium layer. The hydrogenation of 1-hexyne, for example, shows that the supported Pd/PTFE membrane can achieve reaction rates (*e.g.*, 0.71 mmol h^{-1}) which are comparable to 0.92 mmol h^{-1} measured for palladium membranes with a high-surface area palladium electrocatalyst layer. The root cause of these comparable rates is that the high porosity of PTFE enables a 12-fold increase in electrocatalytic surface area compared to planar palladium foil membranes. These results provide a pathway for designing a cost-effective and potentially scalable electrolytic palladium membrane reactor.

Introduction

The electrolysis of water provides a means of converting renewable electricity into dihydrogen fuels.[1–3] The formation of energy dense dihydrogen is particularly appealing for seasonal energy storage and the heavy duty transportation sector, yet the difficulties associated with dihydrogen gas storage and handling continue to constrain the broader deployment of hydrogen fuels.[4,5]

These challenges prompted us to explore alternative ways to utilize cheap and abundant renewable electricity to electrolyze water while bypassing the issues surrounding the management of dihydrogen gas. Our search for such methods drew our attention to electrocatalytic hydrogenation (ECH)[6–12] and electrolytic palladium membrane reactor (PMR) hydrogenation.[13–15] Both methods use electricity to produce protons at an anode sourced from water that are then converted into reactive metal hydride at a cathode. Neither of these methods necessarily provide a solution for using hydrogen as an energy storage medium, but both enable hydrogenation chemistry to be performed using electricity and water.

Electrocatalytic hydrogenation (Fig. 1a) is analogous to conventional chemical hydrogenation (Fig. 1b), but hydrogen is derived from an aqueous or protic electrolyte (*e.g.*, water) rather than dihydrogen gas.[9] Chemical hydrogenation activates dihydrogen gas at a metal surface to create reactive metal hydride that is available for further chemistry.[16] Within an ECH reactor, protons electrolytically produced at an anode migrate to a cathode, where they are reduced to form surface-adsorbed hydrogen. This hydrogen-rich surface is then poised for reaction with unsaturated bonds of organic molecules dissolved in the electrolyte. ECH therefore uses electricity to drive hydrogenation chemistry at ambient pressures and temperatures, without ever requiring gaseous hydrogen.[11,12] Moreover, the hydrogen fugacity can be controlled by the applied electrochemical potential, and a strikingly small applied potential (~0.2–0.3 V) can yield an effective hydrogen pressure of 1000–10 000 atm.[17] While these features are powerful levers for controlling hydrogenation chemistry, ECH must be performed in a protic electrolyte, which fundamentally limits the scope of organic substrates available for chemistry.[9] Confining the organic reactants, products, and electrolyte in the same electrochemical cell also complicates product purification and results in a high solution resistance.

Hydrogenation in a palladium membrane reactor (Fig. 1c) overcomes several limitations of ECH by separating proton

[a]Department of Chemical and Biological Engineering, The University of British Columbia, 2360 East Mall, Vancouver, British Columbia, V6T 1Z3, Canada. E-mail: cberling@chem.ubc.ca

[b]Stewart Blusson Quantum Matter Institute, The University of British Columbia, 2355 East Mall, Vancouver, British Columbia, V6T 1Z4, Canada

[c]Department of Chemistry, The University of British Columbia, 2036 Main Mall, Vancouver, British Columbia, V6T 1Z1, Canada

[d]Canadian Institute for Advanced Research (CIFAR), 661 University Avenue, Toronto, Ontario, M5G 1M1, Canada

† Electronic supplementary information (ESI) available: Additional images and data showing membrane preparation and characterization, electrochemical characterization, and product quantification including Fig. S1–S19 and Table S1. See DOI: 10.1039/c9ta07957b

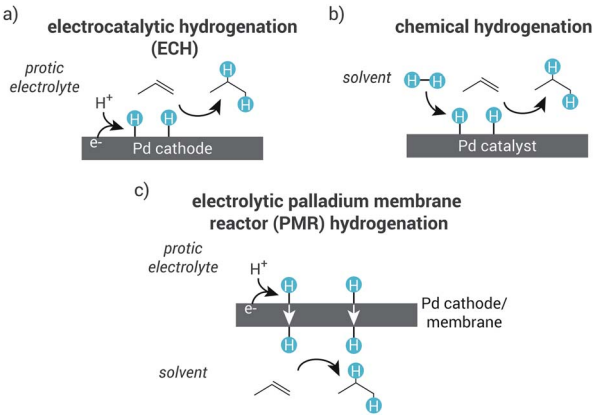

Fig. 1 Types of hydrogenation reactions according to their corresponding hydrogen source and the role of palladium. (a) Electrocatalytic hydrogenation uses protons as a hydrogen source and hydrogenation occurs in protic electrolyte on the same side of the palladium cathode. (b) Chemical hydrogenation uses dihydrogen gas as a hydrogen source and the hydrogenation reaction occurs in any solvent on the same side of the palladium. (c) Electrolytic palladium membrane reactor hydrogenation uses protons from protic electrolyte as a hydrogen source and hydrogenation occurs on the opposing side of the palladium cathode/membrane in any solvent.

reduction in an electrochemical chamber from hydrogenation in a chemical chamber.[13] This architecture is possible because the palladium foil separating the two compartments is selectively permeable to hydrogen atoms.[18] A potential applied to electrodes in the electrochemical chamber produces protons (at the anode) that then migrate to the palladium cathode, where they are reduced to surface-adsorbed hydrogen and then absorbed into the bulk palladium lattice. These hydrogen atoms permeate the palladium membrane to hydrogenate unsaturated organic reactants at the other side of the palladium. The PMR configuration enables palladium to act as a cathode for proton reduction on one side, a catalyst for hydrogenation on the other, and a membrane for permeating hydrogen atoms (Fig. 1c). Unlike ECH, electrolytic palladium membrane hydrogenation can be performed in any solvent (including protic and organic solvents) and therefore substrate scope is not limited by solubility in the reaction medium. Moreover, separating hydrogenation from proton reduction with a palladium membrane bypasses challenges of product purification from protic electrolyte, and results in significant energy savings due to lower solution resistance.[15]

A key shortcoming of an electrolytic PMR, however, is the high cost of the palladium foil.[13–15] While this problem can be addressed by decreasing foil thickness, the mechanical integrity cannot be maintained for membranes with thicknesses <20 μm.[19] This thickness is still too expensive to be economically feasible according to technoeconomic assessments that have shown that a thickness of <15 μm is required for related gas-fed PMR technologies[20–22] (where hydrogen is removed through a palladium membrane) to be cost-competitive with packed-bed reactor dehydrogenation catalysts. Indeed, the membrane reactor catalyst costs >60-fold more than that of the packed-bed reactor, which uses pellets or supported nanoparticles with high surface areas[23,24] and inexpensive supports[20] to reduce palladium content. On this basis, the high catalyst/membrane cost needs to be addressed in order to fully leverage the 4-fold faster reaction rates achieved for the PMR.[25]

The palladium content can be reduced in gas-fed palladium membrane reactors by deposition of thin palladium films onto rigid, porous supports.[26–33] Gas-fed PMRs typically employ rigid materials such as porous glass,[27] alumina,[26,30–32] or stainless steel.[34] Kikuchi, Uemiya, and coworkers have demonstrated that high hydrogen permselectivity is achievable under high temperature and pressure flow conditions using thick (>1 mm), small pore size (<0.1 μm) supports that provide high mechanical strength and thermal resistance.[26–28] These supports also provide good adhesion for the palladium film and enable a pinhole-free palladium membrane.[35] While there have been several studies on supported palladium membranes for gas-fed systems, they may not be amenable to electrolytic PMRs, where solvent and/or electrolyte diffusion to the palladium layer is crucial for reactor success.

We report here that a thin layer of palladium sputter-deposited on a thin, porous polytetrafluoroethylene (PTFE) support is capable of matching the performance of a palladium foil in electrolytic palladium membrane reactors (Fig. 2). We demonstrate that a dense, pinhole-free, 1–2 μm thick palladium layer adheres to the PTFE membrane, and that fast non-polar solvent diffusion occurs through the thin (<100 μm) PTFE support, but does not occur through a thick (<1 mm) porous alumina support. In a proof-of-concept hydrogenation reaction, we show that the Pd/PTFE membrane reduces the mass of palladium used by 20-fold compared to a palladium foil membrane, while maintaining similar 1-hexyne consumption rates of 0.72 mmol h^{-1} (compared to 0.91 mmol h^{-1}). We also resolve the effects of support properties (*e.g.*, pore size, thickness, hydrophobicity), catalytic surface area, and solvent polarity on the membrane design and report on a cost-effective solution for designing supported palladium membranes for electrolytic PMRs.

Experimental section

Materials

Pd 2″ target (99.95%) was purchased from ACI Alloys. Kapton (500 HN) substrates were purchased from American Durafilm. Tetratex Microfiltration PTFE membranes (TX1301, TX1302, TX1325; 8.5″ × 11″) were purchased from Donaldson Membranes. EpoxySet Resin and EpoxySet Hardener were purchased from Allied High Tech Products. A 1 oz wafer bar of Pd (99.95%) was purchased from Silver Gold Bull. $PdCl_2$ (99.9%) was purchased from Strem Chemicals. Porous alumina discs (0.1 μm pore size, 1 mm thickness) were purchased from Coorstek. 1-Hexyne (>97%) was purchased from TCI Chemicals. Pentane (≥99%), DCM (HPLC grade, ≥99.8%), CD_3OD (≥99.8% D), dimethylsulfone (quantitative NMR standard, TraceCERT), MeOH (≥99.8%), HCl (37%), H_2SO_4 (95−98%), CH_3CN (>99.8%), tetrabutylammonium hexafluorophosphate (>99%), and H_2O_2 solution (30 wt% in H_2O) were purchased from Sigma Aldrich. Pt gauze (52 mesh, 99.9%), Pt wire (0.5 mm, 99.95%), 6-chloro-1-hexyne (98%) were purchased from Alfa Aesar. Nitric

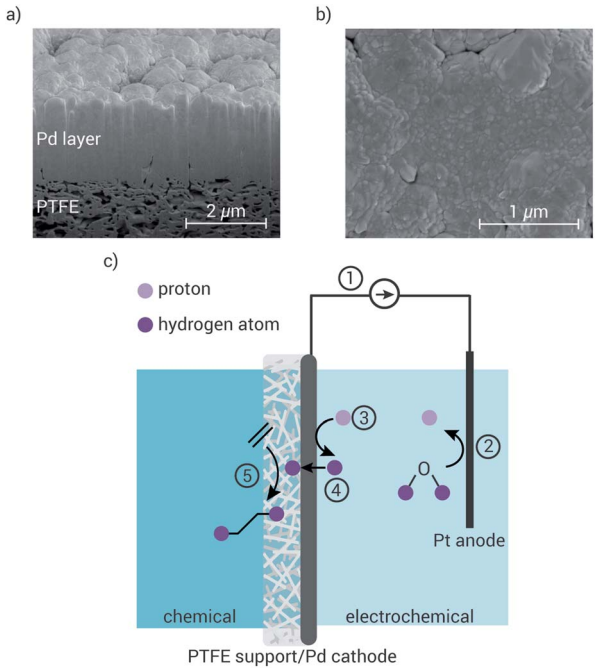

Fig. 2 (a) Cross-sectional and (b) top-view SEM images of a fabricated Pd/PTFE membrane. SEM images show a ~1.9 μm layer of Pd sputtered on a PTFE support. The PTFE support has a 0.05 μm average pore size, 25.4 μm thickness, and 104.7 m^2 g^{-1} BET surface area. (c) Schematic diagram of the electrolytic Pd membrane reactor using a supported Pd/PTFE membrane as a cathode to perform hydrogenation chemistry. A current is applied to the Pd/PTFE cathode (1) and water is oxidized at the Pt anode to form protons (2). Protons are reduced to surface-adsorbed hydrogen at the Pd surface (3), which diffuse through the Pd layer to the chemical compartment (4). In the chemical compartment, the organic reactant diffuses through the porous PTFE support and reacts with surface-adsorbed hydrogen at the Pd–PTFE interface to form hydrogenated products (5).

acid (68–70%) was purchased from VWR. Nafion 117 membranes were purchased from Fuel Cell Store. Ag/AgCl reference electrodes (RE5B) were purchased from BASi. Viton foam gasket ($\frac{1}{8}''$ thickness) was purchased from McMaster Carr.

Materials preparation

PTFE support preparation. A Kapton substrate was cut into two circular 4″ diameter masks each with 16 circular cut outs using a Cricut (Cut Smart 20). A 1 : 1 concentration of EpoxySet Resin and EpoxySet Hardener was combined to make epoxy that was spread on one Kapton mask. Tetratex PTFE was carefully placed on one of the Kapton masks and cured at 120 °C for 24 hours. After 24 hours, epoxy was spread onto the second Kapton mask and the mask was attached to the opposite side of the Tetratex PTFE for mechanical support. The complete PTFE (with Kapton) support (Fig. S1†) was cured at 120 °C for 24 hours and cleaned by sonication in DI water, acetone, and IPA for 1 minute each and then blow-dried with nitrogen gas.

Pd sputter-deposition. Palladium was deposited onto prepared PTFE supports by D.C. magnetron sputtering. The process chamber had a base pressure of 3×10^{-6} torr and an Ar gas working pressure of 1×10^{-3} torr, 2×10^{-3} torr, or 2×10^{-2} torr. Pd deposition was carried out at 100 W after pre-sputtering for 3.5 minutes. The target–substrate distance was 10 cm. The deposition rate was 2.5–3.0 A s^{-1} and resulted in films with thicknesses ranging from 1000–3500 nm. Pd mass was quantified using a Sartorius analytical balance (±0.001 resolution) before and after deposition.

Pd foil preparation. A 1 oz Pd wafer bar was used to roll 1 mm Pd strips that were then annealed at 850 °C for 1.5 hours. The 1 mm strips of Pd were rolled into 25 μm Pd foils and again annealed at 850 °C for 1.5 hours. Thickness of Pd foils were determined by a Mitutoyo digital micrometer. Pd foils were cleaned using a 0.5 : 0.5 : 1 concentration of HNO_3 : H_2O : H_2O_2 solution mixture for ~45 min or until vigorous bubbling subsided. Solution mixture changed from clear to yellow during the cleaning procedure.

Pd catalyst electrodeposition. Pd black catalyst was electrodeposited on the Pd foil (Pd/Pd foil) using a three-compartment cell (*vide infra*). A Pd foil (geometric surface area = 1.22 cm^2) was clamped into the cell as the working electrode and measured against a Ag/AgCl reference electrode. The middle electrochemical compartment was filled with 15.9 mM $PdCl_2$ in 1 M HCl deposition solution and a Pt mesh was placed in the same compartment as the working electrode. The other two compartments were left empty. A potential of −0.2 V *versus* Ag/AgCl was applied to the working electrode until 9 C of charge (7.38 C cm^{-2}) had been passed (~5 mg material). Pd foil mass was quantified using Sartorius analytical balance (±0.001 resolution) before and after electrodeposition.

Liquid diffusion measurements

Liquid diffusion experiments were carried out in a cell with two compartments: one with a solvent inlet and the other with an outlet (Fig. S2†). Prepared PTFE supports and porous alumina supports were sandwiched between the two compartments. Viton foam gaskets were used to seal the support and prevent leaking. The inlet compartment was filled with 5 mL of solvent and measurements of solvent diffusion were made by marking the inlet compartment at regular time intervals. Interval length depended on the solvent and support. Markings for alumina with all solvents, and PTFE with MeOH and H_2O were made every 1–2 hours for 8 hours and at 24 hours. Markings for PTFE with pentane were made every 15 minutes and with DCM every 30 minutes until the inlet compartment was empty.

Scanning electron microscopy (SEM)

Images were acquired with an FEI Helios NanoLab 650 dual beam SEM at 1 kV and 50 pA using a through-lens detector in secondary electron mode. Cross-sectional images were taken at an angle of 52 ° after a focused ion beam was used to evacuate a pit and expose a cross-sectional area. A horizontal field width (HFW) of 5.97 μm was exposed in both cases.

Brunauer–Emmett–Teller (BET) analysis

The BET surface area of the PTFE membrane was determined from N_2 adsorption–desorption on a Micrometrics ASAP 2020 instrument measured at 70 K. Prior to analysis, the PTFE was

pretreated at 373 K under a vacuum pressure of 40 Pa for 8 h to remove any adsorbed moisture from the pores.

Electrochemical measurements

A Metrohm Autolab PGSTAT302N potentiostat and electrolytic palladium membrane reactor were used for electrochemical experiments. The electrolytic palladium membrane reactor used has a three-compartment cell configuration consisting of two electrochemical compartments and one chemical compartment. All three compartments were filled with 35 mL solution volume. The chemical and middle electrochemical compartments were separated by Pd/PTFE (or Pd foil) cathode/working electrode. A Nafion membrane was used between the two electrochemical compartments. Viton foam gaskets were used to seal both the palladium membrane and the Nafion membrane in place and prevent leaking. A Ag/AgCl electrode (3.0 M NaCl) was used as a reference electrode and placed in the middle electrochemical compartment. A 1 cm^2 Pt mesh was used as an anode/counter electrode and placed in the outer electrochemical compartment. The thickness of the Pd layer of the Pd/PTFE cathode was 1–2 μm (or 25 μm for the Pd foil cathode) and the geometric surface area of the cathode was 1.22 cm^2 on both sides. The PTFE support was 25.4 μm thick with 0.05 μm pore size. Experiments were chronopotentiometric where a reductive current was applied by the potentiostat to the Pd/PTFE (or Pd foil) working electrode (cathode) and the potential was measured between the Pd cathode and the reference electrode.

Electrochemically active surface area (ECSA). Electrochemically active surface area (ECSA) measurements of the Pd/PTFE, bare Pd foil, and Pd/Pd foil were performed by running cyclic voltammograms at varying scan rates (10 to 100 mV s^{-1}) and plotting current *versus* scan rate. The middle electrochemical compartment was filled with 0.15 M tetrabutylammonium hexafluorophosphate (TBA-PF_6) in CH_3CN with the other two compartments left empty. A Ag/AgCl reference electrode and Pt mesh counter electrode were used. For Pd/PTFE, double-layer capacitance measurements were done on both sides of the membrane to study the electrochemical surface area at the Pd–PTFE interface and Pd interface. The liquid diffusion of the organic electrolyte through the PTFE layer was confirmed by a relatively low uncompensated resistance of ~95–98 Ω (compared to ~74–76 Ω for Pd foil). A potential range of 0.05 to 0.25 V *versus* Ag/AgCl with the plotted current taken at 0.15 V *versus* Ag/AgCl (the open circuit voltage) was used for all three cases. The slope of the plot was used to measure double-layer capacitance. Specific capacitance was calculated using bare Pd foil because it embodies an atomically smooth planar Pd surface.[36] ECSA was calculated by dividing double-layer capacitance by specific capacitance of Pd to quantify chemical surface area available for reaction.

Atmospheric mass spectrometry (atm-MS). Hydrogen evolution measurements were made using the three-compartment cell with no substrate in the chemical compartment. 1 M H_2SO_4 was added to both electrochemical compartments with a Nafion membrane in between and the solvent in the chemical compartment was changed for each experiment. The Pd/PTFE membrane was placed with the PTFE facing the chemical compartment. Both the chemical and middle electrochemical compartments were attached to the atmospheric mass spectrometer. Both compartments were closed to air and stirred at a consistent rate. The flow rate into the instrument was 10 mL min^{-1}. The potentiostat was used to apply a 100 mA reductive current and an ESS CatalySys atmospheric mass spectrometer was used to measure 2 m/z current ratio over time, switching between the chemical and electrochemical compartment every 2 s with a 5 s purge to detect hydrogen gas evolution on both sides of the cell. The equilibrated ion current values were used to calculate the ratio of chemical : electrochemical hydrogen gas evolution.

Product quantification

Gas chromatography-mass spectrometry (GC-MS). GC-MS was used to quantify products for the hydrogenation of 1-hexyne in pentane and 6-chloro-1-hexyne in pentane and DCM. Aliquots of 300 μL were taken every 2–4 hours during the reaction and diluted in 700 μL pentane or DCM. GC-MS samples were further diluted with 300 μL of dilute reaction mixture with 700 μL pentane or DCM. GC-MS experiments were conducted on an Agilent GC-MS using a HP–5ms column and electron ionization. The prepared samples were run on an autosampler with a 1 μL injection volume and a split ratio of 20 : 1. Reactions in pentane: the oven temperature began at 30 °C for 2 min and ramped to 40 °C at 2 °C min^{-1} then to 200 °C at 40 °C min^{-1}. A solvent delay of 2.15 min was employed. Peaks for 1-hexyne, 1-hexene, n-hexane, 6-chloro-1-hexyne, 6-chloro-1-hexene, and 6-chlorohexane were identified by searching the National Institute of Standards and Technology (NIST) database for matching mass spectra. Reactions in DCM: the oven temperature began at 70 °C for 1 min and ramped to 80 °C at 5 °C min^{-1} and held for 1 min. The temperature was then ramped to 81 °C at 1 °C min^{-1} then to 200 °C at 50 °C min^{-1}. A solvent delay of 2.80 min was employed. Peaks for 6-chloro-1-hexyne, 6-chloro-1-hexene, and 6-chlorohexane were identified by searching the NIST database for matching mass spectra.

Nuclear magnetic resonance (NMR). NMR was used for product quantification of 6-chloro-1-hexyne hydrogenation in MeOH in the chemical compartment. 500 μL of the reaction mixture (0.1 M), 500 μL of methanol-d_4 with 0.1 M dimethylsulfone internal standard were added to an NMR tube. ^1H NMR spectra were acquired on a Bruker Avance 400inv spectrometer at 298 K. Relative concentrations were determined by comparing methylene signals (2H) of 6-chloro-1-hexyne (~1.83 ppm) and 6-chloro-1-hexene (~2.11 ppm) and methyl signal (3H) of 6-chlorohexane (~0.90 ppm). In each case the internal standard was integrated to 6.

Palladium leaching quantification

Inductively coupled plasma-optical emission spectroscopy (ICP-OES). ICP-OES studies were performed with the Pd/PTFE membrane reactor to determine whether any palladium content was leached from the membrane after multiple hydrogenation cycles. The Pd/PTFE membrane was used for three hydrogenation reaction cycles (8 hours per cycle) with 1-hexyne in pentane in the

chemical compartment under an applied current of 50 mA. The sample was prepared by removing the final 30 mL reaction mixture from the chemical compartment after each hydrogenation cycle. Substrate and solvent were removed using a rotary evaporator under vacuum and the vial was treated with 500 μL of 70% HNO_3 for 72 h. Subsequently, 6 mL of dH_2O was added to yield a <5% HNO_3 concentration matrix mixture. A calibration curve was prepared using a 1000 mg L^{-1} Pd in 5% HNO_3 stock standard solution. The calibration curve ranged from 0 to 2.5 ppm with 3 emission lines (340 nm, 361 nm, and 324 nm). ICP-OES measurements of the samples yielded results of 0.021 ± 0.007 ppm for the first cycle, 0.011 ± 0.003 ppm for the second cycle, and 0.014 ± 0.005 ppm for the third cycle in the initial 30 mL reaction mixtures.

Results

Design and fabrication of Pd/PTFE membranes

The supported palladium membranes used in this study were fabricated by sputter-deposition of 1–2 μm of dense palladium onto porous PTFE supports (Fig. 2a and b). PTFE supports were prepared by sealing a PTFE membrane (0.05 μm average pore size, 25.4 μm thickness, 104.7 $m^2 g^{-1}$ BET surface area) between two Kapton masks with circular cutouts with a geometric surface area of 1.22 cm^2 (Fig. S1†). The Pd/PTFE membranes were tested in a three-compartment membrane reactor,[13] and used to separate the two electrochemical compartments from the chemical compartment (Fig. 2c). The Pd/PTFE membrane was configured such that the PTFE support faced the chemical compartment to match the hydrophobicity of the membrane to that of the organic solvents used in the chemical compartment (*vide infra*). The chemical compartment was filled with 35 mL of solvent with or without reactant. The two electrochemical compartments each contained 35 mL of 1 M H_2SO_4 as the electrolyte. A proton-conducting Nafion membrane was used to separate the outer electrochemical compartment containing a 1 cm^2 platinum mesh anode from the middle electrochemical compartment containing a Ag/AgCl reference electrode and the Pd (on PTFE) cathode. In each experiment, a reductive current was applied to the system and protons formed at the Pt anode from water oxidation passed through the Nafion membrane to be reduced to surface-adsorbed hydrogen on the Pd cathode.

Wettability and liquid diffusion experiments

We tested the wettability and liquid diffusion of bare PTFE supports with different pore sizes and thicknesses (pore size, thickness = 0.05 μm, 25.4 μm; 0.1 μm, 74 μm; 0.2 μm, 66 μm) and found that lower-polarity solvents yielded faster liquid diffusion in all cases. Solvent droplet images show a trend in wettability consistent with the polarities of the solvents, with non-polar solvents fully wetting the support (Fig. S3†). Liquid diffusion experiments showed the same trend, where pentane had the fastest diffusion rates of ≥5.5 mL h^{-1} and no H_2O diffused through any of the PTFE supports tested over the 24 hour period (Fig. S2 and Table S1†). Liquid diffusion measurements on porous alumina supports (0.1 μm pore size, 1 mm thickness), commonly used in gas-fed PMRs,[26,30–32] yielded rates of <0.15 mL h^{-1} for all solvents tested. These data show that alumina exhibits slower diffusion rates than PTFE in each case, with the exception of H_2O.

We then tested the effect of depositing a thin palladium film on PTFE supports with different pore sizes and under different sputtering pressures. The amount of palladium required to achieve a pinhole-free, continuous palladium film is dependent on pore size, surface roughness, and surface chemistry of the porous support layer.[33] A 1 μm film of palladium was sputter-deposited onto PTFE supports with 0.05 μm, 0.1 μm, and 0.2 μm pore sizes and palladium surface coverage on each support was examined by SEM (Fig. S4†). SEM images confirmed that a reduction in support pore size resulted in higher palladium surface coverage, and a palladium layer with no visible pinholes >100 nm was obtained using the 0.05 μm pore-sized PTFE support (Fig. 2b and S4a†). A ∼1.5 μm film of palladium was then sputtered using three working pressures: 1×10^{-3} torr, 2×10^{-3} torr, and 2×10^{-2} torr to study the effect of argon pressure on palladium surface morphology. SEM images showed that reducing sputtering pressure resulted in smaller Pd crystals and a more continuous film (Fig. S5†). A pressure of 1×10^{-3} torr resulted in large cracks across the membrane while a pressure of 2×10^{-2} torr did not provide full surface coverage. A sputtering pressure of 2×10^{-3} torr was used for all Pd/PTFE membranes hereafter since it provided a continuous palladium layer without any cracks, which is consistent with observations made for sputter-deposition of thin Pd films on supports in gas-phase systems.[37]

We next performed electrochemical experiments on these dense Pd/PTFE membranes to demonstrate that the hydrophobic PTFE support should be oriented toward the chemical compartment and the palladium toward the electrochemical compartment. The membrane was first tested with the PTFE support facing the electrochemical compartment, and both compartments were filled with 1 M H_2SO_4 (Fig. S6a†). A 100 mA current was applied and the voltage immediately dropped to the −10 V limit of the instrument, suggesting that the electrolyte was not able to diffuse through the PTFE and make contact with the palladium layer. The Pd/PTFE was then reversed such that the PTFE layer faced the chemical side (Fig. S6b†) and a potential of ∼ −0.6 V was recorded over 1 hour (Fig. S6c†). In all experiments hereafter, the Pd/PTFE membrane was orientated such that the PTFE layer faced the chemical side to ensure ionic contact between the electrolyte and the palladium cathode and to ensure PTFE wettability by organic solvents.

Hydrogen permeation measurements

Hydrogen evolution was measured to confirm that the Pd/PTFE membrane was selectively permeable to hydrogen atoms and blocked passage of solvents. For these tests, the electrochemical compartment was filled with 1 M H_2SO_4, the solvent was varied in the chemical compartment, and a 100 mA current was applied (Fig. 3a). An atmospheric-mass spectrometer (atm-MS) was used to measure the relative production of hydrogen gas evolved on the chemical and electrochemical sides of the membrane

(Fig. S7†), with hydrogen flux being defined as the amount of hydrogen gas evolved on chemical side per unit time. Experiments performed with pentane, DCM, MeOH, and H_2SO_4 in the chemical compartment (Fig. 3b and S7†) resulted in 55%, 80%, 88%, and 96%, respectively, of hydrogen gas released on the chemical side, indicating successful hydrogen permeation. Solution resistances did not change before and after the experiments (~4–6 Ω), suggesting that the organic solvent did not pass through the palladium layer in to the electrochemical compartment. These results confirm that only hydrogen (and not solution) permeates the Pd/PTFE membrane in all solvents tested, and that this hydrogen is available for hydrogenation reactions.

Hydrogen permeation measurements were also performed on the Pd/PTFE membranes to study the effect of Pd layer thickness on hydrogen flux. A palladium layer of 1 μm, 1.5 μm, 2 μm, and 3.5 μm was sputter-deposited onto the 0.05 pore-sized PTFE membrane. All Pd thicknesses resulted in a hydrogen flux of ~1.7 mmol cm^{-2} h^{-1}, under 100 mA applied current with 1 M H_2SO_4 in both compartments (Fig. S8†). These data suggest that hydrogen flux is independent of thickness in our Pd/PTFE membrane reactor.

Catalytic hydrogenation measurements

The hydrogenation of 1-hexyne in the chemical compartment of the PMR (Fig. 4a) was used as a proof-of-concept reaction to demonstrate that the Pd/PTFE membrane has comparable reaction rates to a palladium foil with a palladium catalyst layer (Pd/Pd foil) (Fig. 4 and S9). We have previously shown that electrodepositing a layer of palladium black catalyst (~5 mg) onto a planar palladium foil can lead to an increase in catalytic surface area that results in a ~10-fold increase in 1-hexyne consumption rate of Pd/Pd foil compared to Pd foil.[13] In all cases, the chemical compartment was filled with 0.1 M 1-hexyne in pentane, the electrochemical compartment was filled with 1 M H_2SO_4, and a 50 mA current was applied (Fig. 4b and c). We measured the 1-hexyne to be completely consumed after 6 and 8 hours for Pd/Pd foil and Pd/PTFE, respectively (Fig. 4d and e), at

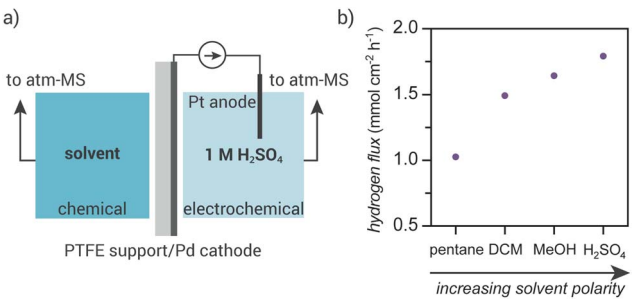

Fig. 3 (a) Electrolytic Pd/PTFE membrane reactor setup to measure hydrogen evolution and flux through the membrane. (b) Hydrogen flux through the palladium layer for solvents with different polarities in the chemical compartment (pentane being the most non-polar and H_2SO_4 being the most polar). A 100 mA current was applied and an atmospheric mass spectrometer (atm-MS) was used to measure H_2 evolved on the chemical and electrochemical sides. Each compartment was filled with 35 mL of solution volume.

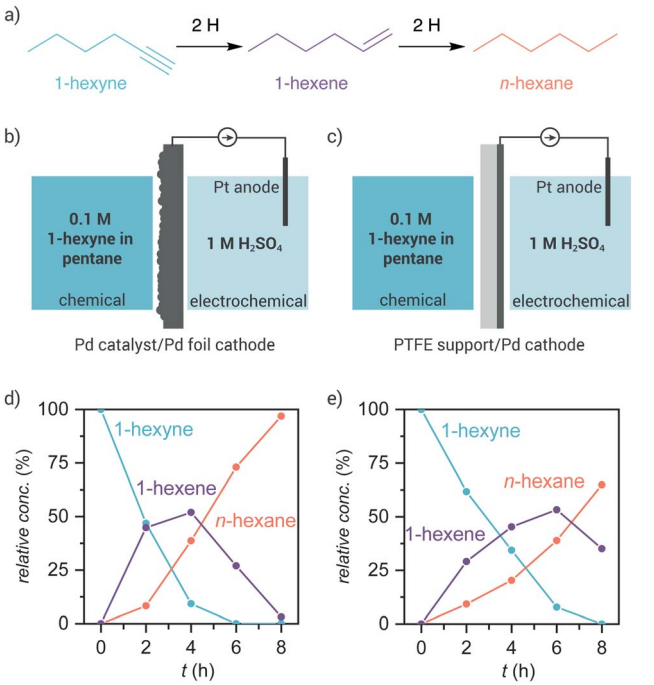

Fig. 4 (a) Hydrogenation reaction of 1-hexyne to 1-hexene and *n*-hexane using (b) electrodeposited palladium catalyst on palladium foil (Pd/Pd foil) membrane and (c) palladium sputtered on PTFE (Pd/PTFE) membrane in the electrolytic palladium membrane reactor. 1-Hexyne consumption and product formation using the (d) Pd/Pd foil membrane and (e) Pd/PTFE membrane over an 8 hour period. Each compartment was filled with 35 mL of solution volume. A 50 mA current was applied in both cases. The Pd foil is 25 μm thick and the Pd layer (of the Pd/PTFE membrane) is 1–2 μm thick.

similar working electrode voltages for both reactors (Fig. S10†). Electrochemical surface area (ECSA) measurements were used as an approximation for the palladium catalytic surface area, and a comparison between a planar Pd foil membrane, Pd/Pd foil, and Pd/PTFE (Fig. S11†) indicated that the catalytic surface areas were 1.22 cm^2, 64.2 cm^2, and 14.9 cm^2 for the three membranes, respectively. These results demonstrate that a supported palladium membrane is effective for hydrogenation in an electrolytic palladium membrane reactor.

Three successive 1-hexyne hydrogenation experiments were performed using a single Pd/Pd foil and Pd/PTFE membrane to measure the stability of the membranes after multiple reaction cycles. For a Pd/Pd foil membrane, the starting 1-hexyne material was consumed after 6 hours during the first two cycles, but took 8 hours to reach completion by the third cycle (Fig. S12a†). The electrodeposited Pd black on the Pd foil was replaced every ≤3 uses to ensure that reaction rates were not affected by any modifications to the catalyst surface. The removal of Pd black using our cleaning procedure (see Experimental), however, reduced the mechanical stability of the palladium foil and over ~3 cleaning procedures, pinholes began to form in the foil rendering it unusable (Fig. S12b and c†). A Pd foil membrane lasts ~9 hydrogenation cycles before it must be replaced with a new foil. The reaction rates also diminished over three hydrogenation cycles for Pd/PTFE

(Fig. S12d†), and after 3–5 cycles the membranes form small cracks and must be replaced (Fig. S12e and f†). The reaction mixtures after each hydrogenation cycle with the Pd/PTFE membrane were analyzed by ICP-OES to determine residual palladium after reaction and no detectable quantities of palladium were found in the chemical compartment. For these tests, 30 mL of 1-hexyne in pentane was used and a palladium concentration of $<21 \pm 7$ ppb was measured at various stages of the reaction with the Pd/PTFE membrane (Fig. S13†).

Hydrogenation experiments were then performed in various solvents to examine how solvent polarity affects reaction rates. The reactant 6-chloro-1-hexyne (Fig. 5a) was used because it could be solubilized in a range of solvents (pentane, DCM, and MeOH). The electrochemical compartment was filled with 1 M H_2SO_4, the solvent was varied in the chemical compartment, and a 50 mA current was applied (Fig. 5b). Experiments were carried out on both Pd/Pd foil and Pd/PTFE to determine if solvent polarity impacted rates of non-supported membranes (Fig. 5c, S14–S17†). Consumption rates of 6-chloro-1-hexyne were determined by the slope of the initial 3 hours of consumption (mmol h^{-1}). Consumption rates were the highest for the most non-polar solvent, pentane (0.58 mmol h^{-1}) and lowest for the most polar solvent, MeOH (0.47 mmol h^{-1}) when Pd/PTFE was used, and 0.6–0.63 mmol h^{-1} for all solvents when Pd/Pd foil was used. These data suggest that the hydrophobicity of the support does affect the hydrogenation reaction and the high hydrophobicity of the PTFE support enables the fastest hydrogenation rates in non-polar solvents.

Discussion

Supports used in gas-fed PMRs that are designed to enable fast hydrogen gas diffusion under high temperature and pressure flow conditions[38] are not necessarily amenable to electrolytic PMRs. In the electrolytic PMR, replacing the Pd foil membrane with Pd deposited on a porous support introduces a resistive layer that reduces how quickly the electrolyte or reactant (depending on membrane orientation) can diffuse through to the palladium catalyst. This extra layer can hinder diffusion rates,[39] negatively impacting the rate of hydrogenation and performance of the reactor. For these reasons, a support layer that enables fast liquid diffusion while providing good adhesion is fundamental to the success of the reactor. Gas-fed studies have shown that sputtering <10 nm of palladium onto an intermediate PTFE support layer (on porous glass) can enable better adhesion than supports without PTFE.[40] Moreover, the liquid diffusion experiments we performed on porous alumina supports show that solvent diffusion rates through the PTFE supports were faster than with the alumina supports in all cases, except for H_2O (Fig. S3 and Table S1†), with a 50-fold increase in rate for the most non-polar solvent (pentane). These data demonstrate that the supported Pd membranes developed up to this point are not amenable for electrolytic PMRs and highlight the importance of developing membranes with thin supports (<200 μm thick) and good liquid diffusion.

The hydrogen flux through the membrane and the 6-chloro-1-hexyne hydrogenation reaction rates were both affected by the polarity of the solvent in the chemical compartment (Fig. 3b and 5c). We attribute both of these effects to the high hydrophobicity and solvent-dependent wettability of the PTFE support (shown schematically in Fig. 6). While 96% of the hydrogen permeated through the Pd when H_2SO_4 was contained in the chemical compartment, merely 55% of hydrogen permeated when pentane was used. Polar solvents like H_2SO_4 (or water) cannot diffuse through the PTFE support, and the PTFE support layer acts effectively as a gas-phase layer (Fig. 6a and S3†). In contrast, pentane fully wets the PTFE support (Fig. 6b and S3†). Hydrogen permeation into the liquid-phase is known to be less favoured than permeation into the gas-phase because a liquid layer can affect both hydrogen transition from bulk to surface and hydrogen recombination at the Pd–PTFE interface.[41]

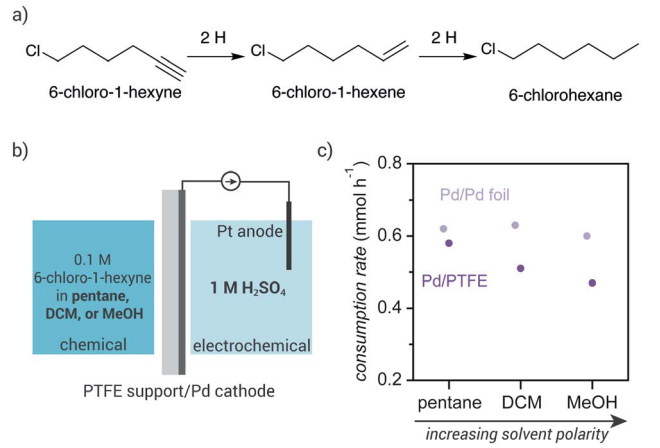

Fig. 5 (a) Hydrogenation reactions of 6-chloro-1-hexyne to 6-chloro-1-hexene and 6-chlorohexane. (b) Cell architecture using the Pd/PTFE membrane reactor and (c) 6-chloro-1-hexyne consumption rates in pentane, DCM, and MeOH with the Pd/Pd foil membrane (light purple) and Pd/PTFE membrane (dark purple). Each compartment was filled with 35 mL of solution volume. A 50 mA current was applied in both cases and consumption rates were determined for the first three hours of reaction.

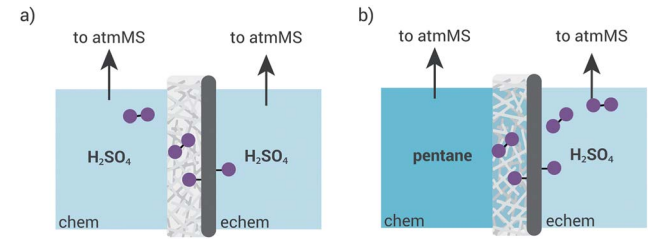

Fig. 6 Schematic depictions of hydrogen flux through the palladium layer demonstrate the difference between (a) a polar solvent (H_2SO_4) and (b) a non-polar solvent (pentane) in the chemical compartment. For a polar solvent, there is no liquid diffusion through the PTFE support which results in a gas-phase PTFE layer that enables hydrogen evolution to occur freely at the palladium-PTFE interface. For a non-polar solvent, liquid diffuses through the PTFE support layer to the palladium-PTFE interface and can affect the rate of hydrogen recombination.

Table 1 Comparison of mass of palladium, electrochemically active surface area, and 1-hexyne consumption rates using palladium foil with palladium catalyst (Pd/Pd foil) and Pd/PTFE membranes in the electrolytic palladium membrane reactor

Membrane	Pd mass (g) ± 0.005	ECSA (cm^2)	Consumption rate (mmol h^{-1})	Normalized consumption rate (mmol g_{Pd}^{-1} h^{-1})
Pd/Pd foil	0.257	64.2	0.91	3.5
Pd/PTFE	0.011	14.9	0.72	65.5

Faster diffusion of non-polar solvents, and therefore the 6-chloro-1-hexyne reactant, to the catalyst surface also enabled faster hydrogenation rates. The hydrogenation rates of 6-chloro-1-hexyne followed a solvent polarity trend (Fig. 5c and S18†), confirming the effect of PTFE wettability in the chemical compartment on hydrogenation rates. These experiments also demonstrated that, even in polar solvents, substrate and solvent can diffuse through the PTFE support to participate in hydrogenation at the palladium layer. Moreover, these findings suggest that the hydrophobicity of the support is an important factor to consider when designing supported membranes for electrolytic PMRs, and that the hydrophobicity of the support needs to be tuned to match the polarity of the solvent/reactant being studied.

Hydrogenation of 1-hexyne proceeded at similar rates using the Pd/PTFE membranes compared to Pd/Pd foil membranes (Fig. 4d and e), with 20-fold less palladium metal. Mass-independent and -dependent (normalized) consumption rates were calculated using the slope of the initial 3 hours of consumption (mmol h^{-1}) divided by mass of palladium content (mmol g_{Pd}^{-1} h^{-1}) (Table 1). The normalized 1-hexyne consumption rates of the Pd/PTFE and Pd/Pd foil membranes were 65.5 mmol g_{Pd}^{-1} h^{-1} and 3.5 mmol g_{Pd}^{-1} h^{-1}, respectively. The 6-chloro-1-hexyne reaction data mirrored these results, with (Fig. S18†) normalized consumption rates of Pd/PTFE >18-fold larger than Pd/Pd foil for all cases. These data indicate that the Pd/PTFE membranes have a significantly higher reaction rate per mass of palladium compared to Pd/Pd foil membranes.

In spite of the fast normalized hydrogenation rates of Pd/PTFE, the measurement of hydrogen flux through Pd/PTFE membranes with different palladium thicknesses showed that hydrogenation rates are independent of palladium thickness. For reactors with the palladium membrane, palladium thickness is inversely proportional to hydrogen permeation only when diffusion is rate-limiting, and reaction rates are independent of thickness when other processes (*e.g.*, absorption into the palladium or hydrogenation on the opposing side of the membrane) are rate-limiting.[42] The data shown in Fig. S8† demonstrates that the hydrogen fluxes are held nearly at parity (~1.7 mmol cm^{-2} h^{-1}) for palladium membrane thicknesses ranging from 1 μm to 3.5 μm. The constant flux at varying thicknesses, as well as the reduction in reaction rate when higher polarity solvents are placed in the chemical compartment (Fig. 3b and 5c), suggest that hydrogenation, and not hydrogen diffusion through palladium, is the rate-limiting step in our Pd/PTFE membrane system.

The comparable consumption rates of 1-hexyne by Pd/PTFE and Pd/Pd foil may be attributed, in part, to the catalytic surface area at the Pd–PTFE interface. ECSA measurements recorded on both sides of the Pd/PTFE membrane show that the catalytic surface area of palladium at the Pd–PTFE interface is ~3× higher than that at the Pd interface (Fig. S19†). The higher ECSA at the Pd–PTFE interface is attributed to the surface structure of the porous PTFE layer, which creates palladium-filled pores (as shown by cross-sectional SEM in Fig. 2a) that result in a non-planar palladium layer. We have previously shown that 1-hexyne hydrogenation rates are affected by catalytic surface area, and that electrodeposition of a palladium catalyst on a planar palladium foil leads to faster reaction rates.[13] The catalytic surface area of the palladium at the Pd–PTFE interface was measured to be 14.9 cm^2 compared to 1.22 cm^2 for planar Pd foil. The higher catalytic surface area of Pd at the Pd–PTFE interface compared to a planar palladium electrode (Fig. S11†) suggests that the surface area is one factor that contributes to the performance of the Pd/PTFE membranes in hydrogenation reactions. These data also indicate that catalytic surface area can be increased by deposition of palladium directly onto a high-surface area porous support without the need for additional catalyst.

Both the Pd/Pd foil and Pd/PTFE membranes have a limited lifetime and must be replaced after a few uses (Fig. S12†). For lab-scale reactions, multiple Pd/PTFE membranes are produced at once (Fig. S1a†), and thus are easier to replace at a reduced cost compared to the Pd foil membranes. The current Pd/PTFE membranes must be replaced due to cracks formed on the Pd surface (Fig. S12f†). The formation of the cracks may be attributed to the expansion and contraction caused by phase transformations of the palladium lattice at room temperature.[33] This situation may be avoided in future studies by alloying palladium with metals such as silver, which improves mechanical stability by reducing phase transformations at room temperature.[26,38,43]

Conclusions

We have demonstrated that a supported Pd/PTFE membrane can reduce the mass of palladium by 20-fold compared to Pd foil membranes in electrolytic palladium membrane reactors. We have shown that supports used in gas-fed reactors are incompatible with the electrolytic environment, and therefore the design of electrolytic PMRs are subject to different constraints compared to gas-fed PMRs. Palladium deposition onto the porous PTFE support enabled a higher catalytic surface area at

the Pd–PTFE interface compared to planar palladium membranes and fast liquid diffusion of organic solvents to the palladium layer. The supported membranes yielded similar hydrogenation rates to palladium foil membranes and improved reaction rates per mass of catalyst. This study shows that supported palladium membranes can be designed to provide a more cost-effective and potentially scalable palladium membrane reactor for electrolytic environments.

Conflicts of interest

There are no conflicts to declare.

Acknowledgements

We are grateful to Stewart Blusson Quantum Matter Institute, the Canadian Natural Science and Engineering Research Council (RGPIN 337345-13), Canadian Foundation for Innovation (229288), Canadian Institute for Advanced Research (BSE-BERL-162173), and Canada Research Chairs for financial support. We thank Brian Ditchburn for fabricating the cells. We also thank Dr Maria Ezhova and Mark Okon for access to the 850 MHz spectrometer, Dr Yun Lung for help with GC-MS experiments, and Majed Alamoudi for help with BET analysis. ICP-OES measurements were performed by Maureen Soon in the Pacific Centre for Isotopic and Geochemical Research. SEM measurements were performed in the Centre for High-Throughput Phenogenomics at the University of British Columbia, a facility supported by the Canada Foundation for Innovation, British Columbia Knowledge Development Foundation, and the UBC Faculty of Dentistry. Sputter-depositions were done at the 4D LABS shared facilities supported by the Canada Foundation for Innovation (CFI), British Columbia Knowledge Development Fund (BCKDF), Western Economic Diversification Canada (WD), and Simon Fraser University (SFU).

References

1 N. S. Lewis and D. G. Nocera, *Proc. Natl. Acad. Sci. U. S. A.*, 2006, **103**, 15729–15735.
2 M. G. Walter, E. L. Warren, J. R. McKone, S. W. Boettcher and Q. Mi, *Chem. Rev.*, 2010, **110**, 6446–6473.
3 V. A. Goltsov and T. N. Veziroglu, *Int. J. Hydrogen Energy*, 2001, **26**, 909–915.
4 R. B. Gupta, *Hydrogen Fuel: Production, Transport, and Storage*, CRC Press, 2008.
5 S. Chu and A. Majumdar, *Nature*, 2012, **488**, 294–303.
6 K. J. Carroll, T. Burger, L. Langenegger, S. Chavez, S. T. Hunt, Y. Román-Leshkov and F. R. Brushett, *ChemSusChem*, 2016, **9**, 1904–1910.
7 Y. Song, U. Sanyal, D. Pangotra, J. D. Holladay, D. M. Camaioni, O. Y. Gutiérrez and J. A. Lercher, *J. Catal.*, 2018, **359**, 68–75.
8 X. H. Chadderdon, D. J. Chadderdon, J. E. Matthiesen, Y. Qiu, J. M. Carraher, J.-P. Tessonnier and W. Li, *J. Am. Chem. Soc.*, 2017, **139**, 14120–14128.
9 J. Lessard, in *Encyclopedia of Applied Electrochemistry*, ed. G. Kreysa, K.-I. Ota and R. F. Savinell, Springer New York, New York, NY, 2014, pp. 443–448.
10 N. Singh, Y. Song, O. Y. Gutiérrez, D. M. Camaioni, C. T. Campbell and J. A. Lercher, *ACS Catal.*, 2016, **6**, 7466–7470.
11 L. Coche and J. C. Moutet, *J. Am. Chem. Soc.*, 1987, **109**, 6887–6889.
12 J. M. Chapuzet, A. Lasia and J. Lessard, *Electrocatalysis*, 1998, 155–159.
13 R. S. Sherbo, R. S. Delima, V. A. Chiykowski, B. P. MacLeod and C. P. Berlinguette, *Nat. Catal.*, 2018, **1**, 501–507.
14 C. Iwakura, Y. Yoshida and H. Inoue, *J. Electroanal. Chem.*, 1997, **431**, 43–45.
15 R. S. Sherbo, A. Kurimoto, C. M. Brown and C. P. Berlinguette, *J. Am. Chem. Soc.*, 2019, **141**, 7815–7821.
16 S. Nishimura, *Handbook of Heterogeneous Catalytic Hydrogenation for Organic Synthesis*, Wiley–VCH, New York, 2001.
17 T. Maoka and M. Enyo, *Electrochim. Acta*, 1981, **26**, 607–614.
18 M. A. V. Devanathan and Z. Stachurski, *Proc. R. Soc. London, Ser. A*, 1962, **270**, 90–102.
19 Y. Kato, K. Inoue, M. Urasaki, S. Tanaka, H. Ninomiya, T. Minagawa, A. Sakurai and J. Ryu, *Proceedings of the International Symposium on Innovative Materials for Processes in Energy Systems* 2010, vol. 2010.
20 M. Sheintuch and D. S. A. Simakov, in *Membrane Reactors for Hydrogen Production Processes*, ed. M. De De Falco, L. Marrelli and G. Iaquaniello, Springer London, London, 2011, pp. 183–200.
21 A. Criscuoli, A. Basile, E. Drioli and O. Loiacono, *J. Membr. Sci.*, 2001, **181**, 21–27.
22 R. D. Dolan and N. C. Dave, *Int. J. Hydrogen Energy*, 2010, **35**, 10994–11003.
23 H. Ramsurn and R. B. Gupta, *New and Future Developments in Catalysis: Chapter 15. Hydrogenation by Nanoparticle Catalysts*, Elsevier Inc. Chapters, 2013.
24 P. N. Rylander, *Organic Syntheses with Noble Metal Catalysts*, Elsevier, 2012.
25 T. Matsuda, I. Koike, N. Kubo and E. Kikuchi, *Appl. Catal., A*, 1993, **96**, 3–13.
26 S. Uemiya, T. Matsuda and E. Kikuchi, *J. Membr. Sci.*, 1991, **56**, 315–325.
27 S. Uemiya, N. Sato, H. Ando, Y. Kude, T. Matsuda and E. Kikuchi, *J. Membr. Sci.*, 1991, **56**, 303–313.
28 S. Uemiya, *Sep. Purif. Methods*, 1999, **28**, 51–85.
29 R. Dittmeyer, V. Höllein and K. Daub, *J. Mol. Catal. A: Chem.*, 2001, **173**, 135–184.
30 S.-I. Niwa, *Science*, 2002, **295**, 105–107.
31 S. Yan, H. Maeda, K. Kusakabe and S. Morooka, *Ind. Eng. Chem. Res.*, 1994, **33**, 616–622.
32 J. Melendez, E. Fernandez, F. Gallucci, M. van Sint Annaland, P. L. Arias and D. A. Pacheco Tanaka, *J. Membr. Sci.*, 2017, **528**, 12–23.
33 S. N. Paglieri and J. D. Way, *Sep. Purif. Methods*, 2002, **31**, 1–169.

34 P. P. Mardilovich, Y. She, Y. H. Ma and M.-H. Rei, *AIChE J.*, 1998, **44**, 310–322.
35 A. J. deRosset, *Ind. Eng. Chem.*, 1960, **52**, 525–528.
36 C. C. L. McCrory, S. Jung, J. C. Peters and T. F. Jaramillo, *J. Am. Chem. Soc.*, 2013, **135**, 16977–16987.
37 K. J. Bryden and J. Y. Ying, *J. Mater. Sci. Eng. A*, 1995, **204**, 140–145.
38 S. Yun and S. Ted Oyama, *J. Membr. Sci.*, 2011, **375**, 28–45.
39 R. E. Beck and J. S. Schultz, *Science*, 1970, **170**, 1302–1305.
40 G. Bramann, B. Zacharias and M. Wienecke, in *Third European Workshop on Optical Fibre Sensors*, International Society for Optics and Photonics, 2007, vol. 6619p. 66191L.
41 N. Itoh and A. M. Sathe, *J. Membr. Sci.*, 1997, **137**, 251–259.
42 T. L. Ward and T. Dao, *J. Membr. Sci.*, 1999, **153**, 211–231.
43 A. G. Knapton, *Platinum Met. Rev.*, 1977, **21**, 44–50.